Journal of Low Temperature Physics, Vol. 139, Nos. 1/2, April 2005 (© 2005)
DOI: 10.1007/s10909-005-3914-3

Impurity Effect on Kramer-Pesch Core Shrinkage in s-Wave Vortex and Chiral p-Wave Vortex

Nobuhiko Hayashi, Yusuke Kato*, and Manfred Sigrist

Institut für Theoretische Physik, ETH-Hönggerberg, CH-8093 Zürich, Switzerland
**Department of Basic Science, University of Tokyo, Tokyo 153-8902, Japan*

The low-temperature shrinking of the vortex core (Kramer-Pesch effect) is studied for an isolated single vortex for chiral p-wave and s-wave superconducting phases. The effect of nonmagnetic impurities on the vortex core radius is numerically investigated in the Born limit by means of a quasiclassical approach. It is shown that in the chiral p-wave phase the Kramer-Pesch effect displays a certain robustness against impurities owing to a specific quantum effect, while the s-wave phase reacts more sensitively to impurity scattering. This suggests chiral p-wave superconductors as promising candidates for the experimental observation of the Kramer-Pesch effect.

PACS numbers: 74.25.Op, 74.20.Rp, 74.70.Pq

1. INTRODUCTION

Much attention has been focused on vortices in nature,[1] especially for the quantized vortex in fermionic superfluid and superconducting systems.[2–4] One of the fundamental physical quantities of the quantized vortex is the radius of vortex core. Kramer and Pesch[5] have pointed out theoretically that the radius of vortex core decreases proportionally to the temperature T at low temperatures, much stronger than anticipated from the temperature dependence of the coherence length. This anomalously strong shrinking of the vortex core, the so-called Kramer-Pesch (KP) effect,[5,6] occurs when the fermionic spectrum of vortex bound states[7–13] crosses the Fermi level.[14] The temperature dependence of the vortex core has been theoretically investigated in the case of superconductors.[9,15–23] The low-temperature limit of the vortex core radius was discussed also for dilute Fermi superfluids[24] and superfluid neutron star matter.[25]

There are several length scales which characterize the radius of vortex

core.[9,25,26] One of them is the coherence length $\xi(T)$. The pair potential $\Delta(r)$ depressed inside the vortex core is restored at a distance $r \sim \xi(T)$ away from the vortex center $r = 0$.[27] However, $\xi(T)$ is almost temperature independent at low temperatures. Another length scale is related to the slope of the pair potential at the vortex center, which is defined as

$$\frac{1}{\xi_1} = \frac{1}{\Delta(r \to \infty)} \lim_{r \to 0} \frac{\Delta(r)}{r}. \tag{1}$$

The KP effect means $\xi_1(T) \propto T$ for $T \to 0$, while the pair potential $\Delta(r)$ is restored at a distance $r \sim \xi$ ($\gg \xi_1$) at low temperatures.[27] Since the spatial profiles of the pair potential $\Delta(r)$ and the supercurrent density $j(r)$ in the vicinity of the vortex center are related with each other through the low-energy vortex bound states, the length ξ_1 scales with the distance $r = r_0$ at which $|j(r)|$ reaches its maximum value.[5,26,28] Therefore, the KP effect gives rise to $r_0 \sim \xi_1 \to 0$ ($T \to 0$) linear in T.

Recently, μSR experiments were performed on the s-wave superconductor $NbSe_2$ to observe the KP effect.[26,28–30] The experimental data of spin precessions, which correspond to the Fourier transformation of the Redfield pattern (the magnetic field distribution) of a vortex lattice, are fitted by a theoretical formula,[31] extracting the information on the spatial profile of the supercurrent density $j(r)$ around vortices.[26,28] While a shrinking vortex core was observed, it was weaker than the theoretical expectation of the KP effect for a clean superconductor. That is, indeed the observed vortex core radius r_0 seemingly shrank linearly in T, but was extrapolated towards a finite value in zero-temperature limit, indicating a saturation of the KP core shrinkage at a low temperature. The measurement of the vortex core radius r_0 by μSR was also performed for $CeRu_2$ with a similar result.[32] Since the KP effect is directly connected with the low-energy vortex bound states, the energy level broadening due to impurities may give rise to a modification of the KP effect,[5] in particular, a saturation as observed. Impurities exist inevitably in any solid state material, so that such a saturation effect is not unlikely to occur. Even it turns out that a rather small concentration of impurities, leaving the material moderately clean, would have a strong influence as observed in experiments.[26,28–30,32]

There are several factors which influence the behavior of vortex core radius. (i) Impurity effects.[5] (ii) The discreteness of the energy levels of the vortex bound states.[5,20–22] (iii) Vortex lattice effects.[26,28,33–37] (iv) Fermi liquid effects F_1^s.[38] (v) Antiferromagnetic correlations induced inside the vortex core as suggested for cuprate superconductors.[39] (vi) The presence of multiple gaps in multi-band superconductors.[40,41]

In this paper, we investigate the temperature dependence of the vortex core radius $\xi_1(T)$ incorporating the effect of nonmagnetic impurities on the

level of the Born approximation, for both a chiral p-wave and an s-wave superconductor. For this purpose, we set up a model of single vortex in a two-dimensional superconductor, where the chiral p-wave pairing has the form[42,43] $\mathbf{d}(\bar{\mathbf{k}}) = \bar{\mathbf{z}}(\bar{k}_x \pm i\bar{k}_y)$ as, for example, realized in Sr_2RuO_4.

The examination of the temperature dependence of $\xi_1(T)$ suggests that under certain conditions the chiral p-wave state shows a more robust KP effect against impurities than an s-wave state. This behavior is connected with the compensation of the intrinsic phase structure and the vortex phase winding, if chirality and phase winding are oppositely oriented.[23,44–52] Therefore, we argue that chiral p-wave superconductors might be better candidates for the experimental observation of the KP effect. The chiral p-wave superconductivity has been proposed for Sr_2RuO_4 with rather strong experimental evidence,[42,43] and more recently for $Na_xCoO_2 \cdot yH_2O$.[53,54]

The paper is organized as follows. In Sec. 2, the self-consistent system of equations for the superconducting order parameter and the impurity self energy is formulated on the basis of the quasiclassical theory of superconductivity. In Sec. 3, the systems of the s-wave vortex and the chiral p-wave vortex are described. The numerical results for the vortex core radius $\xi_1(T)$ are shown in Sec. 4. The summary is given in Sec. 5.

2. QUASICLASSICAL THEORY

Our theoretical analysis of the KP effect will be based on the quasiclassical theory of superconductivity,[55,56] which allows us to take inhomogeneous structures as a vortex into account and at the same time to deal with impurity scattering on a straightforward way.

We start with the quasiclassical Green function in the presence of nonmagnetic impurities,

$$\hat{g}(i\omega_n, \mathbf{r}, \bar{\mathbf{k}}) = -i\pi \begin{pmatrix} g & if \\ -if^\dagger & -g \end{pmatrix}, \tag{2}$$

which is the solution of the Eilenberger equation

$$i\mathbf{v}_\mathrm{F}(\bar{\mathbf{k}}) \cdot \nabla \hat{g} + [i\omega_n \hat{\tau}_3 - \hat{\Delta} - \hat{\sigma}, \hat{g}] = 0. \tag{3}$$

Here, $\hat{\Delta}$ is the superconducting order parameter

$$\hat{\Delta}(\mathbf{r}, \bar{\mathbf{k}}) = \begin{pmatrix} 0 & \Delta \\ -\Delta^* & 0 \end{pmatrix}, \tag{4}$$

and $\hat{\sigma}$ denotes the self energy correction due to impurity scattering

$$\hat{\sigma}(i\omega_n, \mathbf{r}, \bar{\mathbf{k}}) = \begin{pmatrix} \sigma_{11} & \sigma_{12} \\ \sigma_{21} & \sigma_{22} \end{pmatrix}. \tag{5}$$

The Eilenberger equation is supplemented by the normalization condition $\hat{g}(i\omega_n, \mathbf{r}, \bar{\mathbf{k}})^2 = -\pi^2 \hat{1}$.[55,56] The vector $\mathbf{r}$ is the real-space coordinates and the unit vector $\bar{\mathbf{k}}$ represents the sense of the wave number on the Fermi surface. $\mathbf{v}_{\mathrm{F}}(\bar{\mathbf{k}})$ is the Fermi velocity, $\omega_n = \pi T(2n+1)$ is the fermionic Matsubara frequency (with the temperature T and the integer n), $\hat{\tau}_3$ is the third Pauli matrix in the 2×2 particle-hole space, and the commutator $[\hat{a}, \hat{b}] = \hat{a}\hat{b} - \hat{b}\hat{a}$. We will consider an isolated single vortex in extreme type-II superconductors (Ginzburg-Landau parameter $\kappa \gg 1$), and therefore the vector potential is neglected in the Eilenberger equation (3). Throughout the paper, vectors with the upper bar denote unit vectors and we use units in which $\hbar = k_{\mathrm{B}} = 1$.

We now define an alternative impurity self energy $\hat{\Sigma}$ as

$$\hat{\Sigma}(i\omega_n, \mathbf{r}, \bar{\mathbf{k}}) = \begin{pmatrix} \Sigma_{\mathrm{d}} & \Sigma_{12} \\ \Sigma_{21} & -\Sigma_{\mathrm{d}} \end{pmatrix} = \begin{pmatrix} \frac{1}{2}(\sigma_{11} - \sigma_{22}) & \sigma_{12} \\ \sigma_{21} & -\frac{1}{2}(\sigma_{11} - \sigma_{22}) \end{pmatrix}. \tag{6}$$

The original impurity self energy (5) can be expressed as

$$\hat{\sigma} = \hat{\Sigma} + \frac{\sigma_{11}}{2}\hat{1} + \frac{\sigma_{22}}{2}\hat{1}. \tag{7}$$

Hence, we rewrite the Eilenberger equation (3) as

$$i\mathbf{v}_{\mathrm{F}}(\bar{\mathbf{k}}) \cdot \nabla \hat{g} + [i\tilde{\omega}_n \hat{\tau}_3 - \hat{\tilde{\Delta}}, \hat{g}] = 0, \tag{8}$$

with the renormalized Matsubara frequency

$$i\tilde{\omega}_n = i\omega_n - \Sigma_{\mathrm{d}}, \tag{9}$$

and the renormalized superconducting order parameter

$$\hat{\tilde{\Delta}} = \begin{pmatrix} 0 & \Delta + \Sigma_{12} \\ -(\Delta^* - \Sigma_{21}) & 0 \end{pmatrix}. \tag{10}$$

We restrict here to s-wave scattering at the impurities. The single-impurity t-matrix[57] is then calculated as

$$\hat{t}(i\omega_n, \mathbf{r}) = v\hat{1} + N_0 v \Big\langle \hat{g}(i\omega_n, \mathbf{r}, \bar{\mathbf{k}}) \Big\rangle \hat{t}(i\omega_n, \mathbf{r}), \tag{11}$$

where v is the impurity potential for the s-wave scattering channel, N_0 is the normal-state density of states at the Fermi level, and the brackets $\langle \cdots \rangle$ denote the average over the Fermi surface. The impurity self energy $\hat{\sigma}$ is given by

$$\hat{\sigma}(i\omega_n, \mathbf{r}) = n_{\mathrm{i}} \hat{t}(i\omega_n, \mathbf{r}) = \frac{n_{\mathrm{i}} v}{D} \Big[\hat{1} + N_0 v \Big\langle \hat{g}(i\omega_n, \mathbf{r}, \bar{\mathbf{k}}) \Big\rangle \Big], \tag{12}$$

where the denominator is

$$D = 1 + (\pi N_0 v)^2[\langle g\rangle^2 + \langle f\rangle\langle f^\dagger\rangle], \tag{13}$$

and $n_{\rm i}$ is the density of impurities. The scattering phase shift δ_0 is defined by $\tan\delta_0 = -\pi N_0 v$. In this paper, we investigate the Born limit ($\delta_0 \ll 1$). The impurity self energy (12) in this limit becomes

$$\begin{aligned}\hat{\sigma}(i\omega_n, \mathbf{r}) &= n_{\rm i} v \hat{1} + \frac{\Gamma_{\rm n}}{\pi}\Big\langle \hat{g}(i\omega_n, \mathbf{r}, \bar{\mathbf{k}})\Big\rangle \\ &= n_{\rm i} v \hat{1} + \Gamma_{\rm n}\begin{pmatrix} -i\langle g\rangle & \langle f\rangle \\ -\langle f^\dagger\rangle & i\langle g\rangle \end{pmatrix},\end{aligned} \tag{14}$$

where we have defined the impurity scattering rate in the normal state as $\Gamma_{\rm n} = 1/2\tau_{\rm n} = \pi n_{\rm i} N_0 v^2$. The mean free path l is defined by $l = v_{\rm F}\tau_{\rm n} = v_{\rm F}/2\Gamma_{\rm n}$. From Eqs. (6) and (14), we obtain the self-consistency equations for $\hat{\Sigma}$ as

$$\Sigma_{\rm d}(i\omega_n, \mathbf{r}) = -i\Gamma_{\rm n}\Big\langle g(i\omega_n, \mathbf{r}, \bar{\mathbf{k}})\Big\rangle, \tag{15}$$

$$\Sigma_{12}(i\omega_n, \mathbf{r}) = \Gamma_{\rm n}\Big\langle f(i\omega_n, \mathbf{r}, \bar{\mathbf{k}})\Big\rangle, \tag{16}$$

$$\Sigma_{21}(i\omega_n, \mathbf{r}) = -\Gamma_{\rm n}\Big\langle f^\dagger(i\omega_n, \mathbf{r}, \bar{\mathbf{k}})\Big\rangle. \tag{17}$$

The self-consistency equation for Δ, called gap equation, is given as

$$\Delta(\mathbf{r}, \bar{\mathbf{k}}) = \pi T g F(\bar{\mathbf{k}}) \sum_{-\omega_{\rm c}<\omega_n<\omega_{\rm c}} \Big\langle F^*(\bar{\mathbf{k}}') f(i\omega_n, \mathbf{r}, \bar{\mathbf{k}}')\Big\rangle, \tag{18}$$

where the cutoff energy is $\omega_{\rm c}$, the pairing interaction is defined as $gF(\bar{\mathbf{k}})F^*(\bar{\mathbf{k}}')$ with the coupling constant g given by

$$\frac{1}{g} = \ln\Big(\frac{T}{T_{\rm c0}}\Big) + \sum_{0\le n<(\omega_{\rm c}/\pi T-1)/2} \frac{2}{2n+1}. \tag{19}$$

We define $T_{\rm c0}$ as the superconducting critical temperature in the absence of impurities. Finally, the system of equations to be solved consists of the Eilenberger equation (8) and the self-consistency equations for the impurity self-energies [Eqs. (15)–(17)] and for the superconducting order parameter [Eq. (18)].

3. S-WAVE AND CHIRAL P-WAVE VORTEX SYSTEMS

In this study, the system is assumed to be an isotropic two-dimensional conduction layer perpendicular to the vorticity along the z axis. In the circular coordinate system we use $\mathbf{r} = (r\cos\phi, r\sin\phi)$ and $\bar{\mathbf{k}} = (\cos\theta, \sin\theta)$. We assume a circular Fermi surface and $\mathbf{v}_{\rm F}(\bar{\mathbf{k}}) = v_{\rm F}\bar{\mathbf{k}} = (v_{\rm F}\cos\theta, v_{\rm F}\sin\theta)$ in the Eilenberger equations (3) and (8). The average over the Fermi surface reads: $\langle\cdots\rangle = \int_0^{2\pi}\cdots d\theta/2\pi$.

3.1. Pair Potential

The single vortex is situated at the origin $\mathbf{r} = 0$. In the case of the s-wave pairing, the pair potential (i.e., the superconducting order parameter) around the vortex is expressed as

$$\Delta_{\rm s}(\mathbf{r}) = \Delta_{\rm s}(r)e^{i\phi}, \tag{20}$$

where we can take $\Delta_{\rm s}(r)$ in the right-hand side to be real because of axial symmetry of the system. The s-wave pairing means $F(\bar{\mathbf{k}}) = 1$ and the gap equation (18) reads:

$$\Delta_{\rm s}(\mathbf{r}) = \pi T g_{\rm s} \sum_{-\omega_{\rm c}<\omega_n<\omega_{\rm c}} \int_0^{2\pi} \frac{d\theta}{2\pi} f(i\omega_n, \mathbf{r}, \theta), \tag{21}$$

where $g_{\rm s}$ follows Eq. (19).

On the other hand, in the case of the chiral p-wave pairing, $F(\bar{\mathbf{k}}) = \bar{k}_x \pm i\bar{k}_y = \exp(\pm i\theta)$. The pair potential around the vortex has two possible forms depending on whether the chirality and vorticity are parallel or antiparallel each other.[23,51,52] Thus, there are two kinds of vortex. One form is

$$\begin{aligned}\Delta^{(\rm n)}(\mathbf{r},\theta) &= \Delta_+^{(\rm n)}(\mathbf{r})e^{+i\theta} + \Delta_-^{(\rm n)}(\mathbf{r})e^{-i\theta} \\ &= \Delta_+^{(\rm n)}(r)e^{i(\theta-\phi)} + \Delta_-^{(\rm n)}(r)e^{i(-\theta+\phi)},\end{aligned} \tag{22}$$

where the chirality (related to the phase "$+\theta$") and vorticity ("$-\phi$") are antiparallel ("negative vortex"). The other form is

$$\begin{aligned}\Delta^{(\rm p)}(\mathbf{r},\theta) &= \Delta_+^{(\rm p)}(\mathbf{r})e^{+i\theta} + \Delta_-^{(\rm p)}(\mathbf{r})e^{-i\theta} \\ &= \Delta_+^{(\rm p)}(r)e^{i(\theta+\phi)} + \Delta_-^{(\rm p)}(r)e^{i(-\theta+3\phi)},\end{aligned} \tag{23}$$

where the chirality ("$+\theta$") and vorticity ("$+\phi$") are parallel ("positive vortex"). We have assumed that $\Delta_+^{(\rm n,p)}$ is the dominant component in both Eqs.

(22) and (23), and the other component $\Delta_{-}^{(\mathrm{n,p})}$ is the minor one induced with smaller amplitudes inside the vortex core. The axial symmetry allows us to take $\Delta_{\pm}^{(\mathrm{n,p})}(r)$ to be real in each second line of Eqs. (22) and (23). Far away from the vortex, the dominant component $\Delta_{+}^{(\mathrm{n,p})}(r \to \infty)$ is finite and the induced minor one $\Delta_{-}^{(\mathrm{n,p})}(r \to \infty) \to 0$, namely

$$\Delta^{(\mathrm{n})}(r \to \infty, \phi; \theta) = \Delta_{+}^{(\mathrm{n})}(r \to \infty) e^{i(\theta - \phi)}, \tag{24}$$

$$\Delta^{(\mathrm{p})}(r \to \infty, \phi; \theta) = \Delta_{+}^{(\mathrm{p})}(r \to \infty) e^{i(\theta + \phi)}. \tag{25}$$

In the clean limit, $\Delta_{+}^{(\mathrm{n,p})}(r \to \infty) = \Delta_{\mathrm{BCS}}(T)$ [$\Delta_{\mathrm{BCS}}(T)$ is the BCS gap amplitude]. The gap equation (18) reads now:

$$\Delta_{\pm}^{(\mathrm{n,p})}(\mathbf{r}) = \pi T g_{\mathrm{p}} \sum_{-\omega_{\mathrm{c}} < \omega_n < \omega_{\mathrm{c}}} \int_0^{2\pi} \frac{d\theta}{2\pi} e^{\mp i\theta} f(i\omega_n, \mathbf{r}, \theta), \tag{26}$$

where g_{p} follows Eq. (19).

3.2. Axial Symmetry and Boundary Condition

The numerical calculation of the self-consistent pair potential Δ and impurity self energy $\hat{\Sigma}$ requires to restrict ourselves to a finite spatial region, which we choose axial symmetric with a cutoff radius r_{c}. Therefore, it is necessary to fix the values of Δ and $\hat{\Sigma}$ for $r > r_{\mathrm{c}}$ outside the boundary $r = r_{\mathrm{c}}$ when solving the Eilenberger equation (8).

We set, for the pair potential (20) of the s-wave vortex,

$$\Delta_{\mathrm{s}}(r > r_{\mathrm{c}}, \phi) = \Delta_{\mathrm{s}}(r = r_{\mathrm{c}}) e^{i\phi}. \tag{27}$$

For the pair potential (22) of the chiral negative p-wave vortex, we set

$$\Delta^{(\mathrm{n})}(r > r_{\mathrm{c}}, \phi; \theta) = \Delta_{+}^{(\mathrm{n})}(r = r_{\mathrm{c}}) e^{i(\theta - \phi)}, \tag{28}$$

and for the pair potential (23) of the chiral positive p-wave vortex

$$\Delta^{(\mathrm{p})}(r > r_{\mathrm{c}}, \phi; \theta) = \Delta_{+}^{(\mathrm{p})}(r = r_{\mathrm{c}}) e^{i(\theta + \phi)}, \tag{29}$$

while $\Delta_{-}^{(\mathrm{n,p})}(r > r_{\mathrm{c}}) = 0$.

Next we consider the symmetry property and boundary condition of the impurity self energy $\hat{\Sigma}$. In the Eilenberger equation (8), $\hat{\Sigma}$ appears in Eqs. (9) and (10) in the form of $i\omega_n - \Sigma_{\mathrm{d}}$, $\Delta + \Sigma_{12}$, and $\Delta^* - \Sigma_{21}$. Owing to the

axial symmetry of our model, an axial rotation of the system ($\phi \to \phi + \alpha$ and $\theta \to \theta + \alpha$) leads to a transformation of the impurity self energies $\Sigma_{\rm d}$, Σ_{12}, and Σ_{21} in the same manner as $i\omega_n$, Δ, and Δ^*, respectively. The Matsubara frequency $i\omega_n$ is invariant under the axial rotation, and therefore $\Sigma_{\rm d}(i\omega_n, r, \phi)$ has no azimuthal ϕ dependence. Hence, we set

$$\Sigma_{\rm d}(i\omega_n, r, \phi) = \Sigma_{\rm d}(i\omega_n, r), \tag{30}$$

$$\Sigma_{\rm d}(i\omega_n, r > r_{\rm c}) = \Sigma_{\rm d}(i\omega_n, r = r_{\rm c}), \tag{31}$$

both in the case of the s-wave vortex and the chiral p-wave vortex.

For the s-wave vortex, the pair potential $\Delta_{\rm s}(\mathbf{r})$ in Eq. (20) transforms under an axial rotation as $\Delta_{\rm s}(r, \phi+\alpha) = \Delta_{\rm s}(r) \exp[i(\phi+\alpha)] = \Delta_{\rm s}(r, \phi) \exp(i\alpha)$, and $\Delta_{\rm s}^*(r, \phi+\alpha) = \Delta_{\rm s}^*(r, \phi) \exp(-i\alpha)$. This rotation means that $\Delta_{\rm s} + \Sigma_{12} \to (\Delta_{\rm s} + \Sigma_{12}) \exp(i\alpha)$ and $\Delta_{\rm s}^* - \Sigma_{21} \to (\Delta_{\rm s}^* - \Sigma_{21}) \exp(-i\alpha)$. Thus, the off-diagonal impurity self energies $\Sigma_{12,21}(i\omega_n, r, \phi)$ have to possess an azimuthal ϕ dependence as

$$\Sigma_{12}(i\omega_n, r, \phi) = \Sigma_{12}(i\omega_n, r) \exp(i\phi), \tag{32}$$

$$\Sigma_{21}(i\omega_n, r, \phi) = \Sigma_{21}(i\omega_n, r) \exp(-i\phi). \tag{33}$$

We set, for the s-wave vortex, the boundary condition as

$$\Sigma_{12}(i\omega_n, r > r_{\rm c}) = \Sigma_{12}(i\omega_n, r = r_{\rm c}), \tag{34}$$

$$\Sigma_{21}(i\omega_n, r > r_{\rm c}) = \Sigma_{21}(i\omega_n, r = r_{\rm c}), \tag{35}$$

because far away from the vortex core the anomalous Green functions averaged over the Fermi surface, which appear in Eqs. (16) and (17), are generally nonzero and their amplitudes are spatially uniform, owing to the s-wave pairing symmetry.[48]

For the chiral negative p-wave vortex, the pair potential $\Delta^{(\rm n)}$ has the following symmetry properties. For an axial rotation, the pair potential $\Delta^{(\rm n)}(\mathbf{r}, \theta)$ in Eq. (22) transforms as $\Delta^{(\rm n)}(r, \phi+\alpha; \theta+\alpha) = \Delta^{(\rm n)}(r, \phi; \theta)$ and $\Delta^{(\rm n)*}(r, \phi+\alpha; \theta+\alpha) = \Delta^{(\rm n)*}(r, \phi; \theta)$, namely invariant. Therefore, we find that $\Delta^{(\rm n)} + \Sigma_{12} \to \Delta^{(\rm n)} + \Sigma_{12}$ and $\Delta^{(\rm n)*} - \Sigma_{21} \to \Delta^{(\rm n)*} - \Sigma_{21}$ and the off-diagonal impurity self energies $\Sigma_{12,21}(i\omega_n, r, \phi)$ are not ϕ-dependent:

$$\Sigma_{12}(i\omega_n, r, \phi) = \Sigma_{12}(i\omega_n, r), \tag{36}$$

$$\Sigma_{21}(i\omega_n, r, \phi) = \Sigma_{21}(i\omega_n, r). \tag{37}$$

We set, for the chiral negative p-wave vortex, the boundary condition as

$$\Sigma_{12}(i\omega_n, r > r_{\rm c}) = 0, \tag{38}$$

$$\Sigma_{21}(i\omega_n, r > r_c) = 0, \tag{39}$$

because far away from the vortex core the anomalous Green functions averaged over the Fermi surface are zero, owing to the p-wave pairing symmetry.[48]

On the other hand, the chiral positive p-wave vortex behaves differently under axial rotation. The pair potential $\Delta^{(p)}(\mathbf{r}, \theta)$ in Eq. (23) transforms as $\Delta^{(p)}(r, \phi + \alpha; \theta + \alpha) = \Delta^{(p)}(r, \phi; \theta) \exp(2i\alpha)$ and $\Delta^{(p)*}(r, \phi + \alpha; \theta + \alpha) = \Delta^{(p)*}(r, \phi; \theta) \exp(-2i\alpha)$, such that $\Delta^{(p)} + \Sigma_{12} \to (\Delta^{(p)} + \Sigma_{12}) \exp(2i\alpha)$ and $\Delta^{(p)*} - \Sigma_{21} \to (\Delta^{(p)*} - \Sigma_{21}) \exp(-2i\alpha)$. Here, the off-diagonal impurity self energies $\Sigma_{12,21}(i\omega_n, r, \phi)$ depends on ϕ like

$$\Sigma_{12}(i\omega_n, r, \phi) = \Sigma_{12}(i\omega_n, r) \exp(2i\phi), \tag{40}$$

$$\Sigma_{21}(i\omega_n, r, \phi) = \Sigma_{21}(i\omega_n, r) \exp(-2i\phi). \tag{41}$$

We set, for the chiral positive p-wave vortex, the boundary condition as

$$\Sigma_{12}(i\omega_n, r > r_c) = 0, \tag{42}$$

$$\Sigma_{21}(i\omega_n, r > r_c) = 0, \tag{43}$$

as in the case of the negative vortex.

4. VORTEX CORE RADIUS $\xi_1(T)$

The vortex core radius $\xi_1(T)$ defined in Eq. (1) is obtained from the spatial profile of the pair potential calculated self-consistently. We solve the Eilenberger equation (8) by a method of the Riccati parametrization,[10,58] and then iterate the calculation, until self-consistency is reached, with the self-consistency equations of the impurity self energies [Eqs. (15)–(17)] and that of the pair potential for the s-wave vortex [Eq. (21)] or for the chiral p-wave vortices [Eq. (26)]. We use an acceleration method for iterative calculations to obtain sufficient accuracy.[59] When solving the Eilenberger equation (8), we use the boundary conditions for the pair potential and the impurity self energies described in Sec. 3.2.

We show now the results of $\xi_1(T)$ for the three cases introduced above. We set the cutoff energy $\omega_c = 10\Delta_0$ and the cutoff length $r_c = 10\xi_0$. Here, Δ_0 is the BCS gap amplitude at zero temperature in the absence of impurities, and $\xi_0 = v_F/\Delta_0$. The lowest value of the temperature at which ξ_1 is computed is $T = 0.02T_{c0}$.

We have checked an influence of the finite system size, comparing results of ξ_1 obtained for two cutoff lengths $r_c = 10\xi_0$ and $20\xi_0$ in the case of the clean limit. As a result, it was found that those results well coincide each

other below $T \sim 0.7T_{c0}$ (the deviations in ξ_1 are less than $0.003\xi_0$ and negligibly small), while slight deviations appear above $T \sim 0.8T_{c0}$, but are less than $0.014\xi_0$ ($T \leq 0.9T_{c0}$) and almost invisible for plots with the same plot scale as in the following figures.

4.1. S-Wave Vortex

In Fig. 1, we show the vortex core radius $\xi_1(T)$ for the s-wave vortex as a function of the temperature T for several values of the impurity scattering rate Γ_n. The critical temperature T_c remains unaffected by the nonmagnetic impurities, namely $T_c = T_{c0}$ for any values of Γ_n.

At high temperatures, we see in Fig. 1 that the vortex core radius ξ_1 decreases with the increase of the impurity scattering rate Γ_n. This is because the coherence length ξ, over which the pair potential significantly changes, shrinks with the decrease of the quasiparticle mean free path ($\propto 1/\Gamma_n$).[60] The coherence length ξ is a distance at which the pair potential is restored far away from the vortex center. The vortex core radius ξ_1 defined in the vicinity of the vortex center is dominated by this Γ_n dependence of the coherence length ξ in this temperature regime.

Pronounced Γ_n dependence appears also at low temperatures. For $\Gamma_n = 0$ (the clean limit), the vortex core radius ξ_1 decreases linearly in T, as expected for the KP effect. In Fig. 1(a), we also show $\xi_1(T)$ for finite values of the impurity scattering rate, $\Gamma_n = 0.1\Delta_0$ and Δ_0. At low temperatures, the vortex core radius ξ_1 *increases* with the increase of Γ_n, in contrast to the high-temperature behavior. This increase of ξ_1 indicates the saturation feature of the KP effect due to impurities.[5] The low-temperature vortex core radius ξ_1 expands by introducing impurity scattering but still remains much smaller than ξ. For relatively small Γ_n ($< \Delta_0$), the decrease of the coherence length ξ mentioned above has little influence on this expansion of the vortex core radius ξ_1 ($\ll \xi$). For larger Γ_n towards the dirty limit, however, the decrease of the coherence length ξ begins to influence the vortex core radius ξ_1, and ξ_1 begins to decrease with growing Γ_n as seen in Fig. 1(b).

In Fig. 1(b) the solid line displays the function $1/\tanh(1.74\sqrt{(T_c/T)-1})$ $\approx \Delta_0/\Delta_{BCS}(T) = v_F/\Delta_{BCS}(T)\xi_0$. In the dirty case ($\Gamma_n = 10\Delta_0$, i.e., the mean free path $l = v_F/2\Gamma_n = 0.05\xi_0$), $\xi_1(T)$ behaves like the clean-limit BCS coherence length $\sim v_F/\Delta_{BCS}(T)$ below $T \sim 0.6T_c$, and is almost constant at low temperatures. The increase of the vortex core radius $\xi_1(T)$ with increasing T at high temperatures for the dirty case $\Gamma_n = 10\Delta_0$, is more gradual than the temperature dependence of the clean-limit BCS coherence length (the solid line in Fig. 1(b)). This behavior is qualitatively consistent

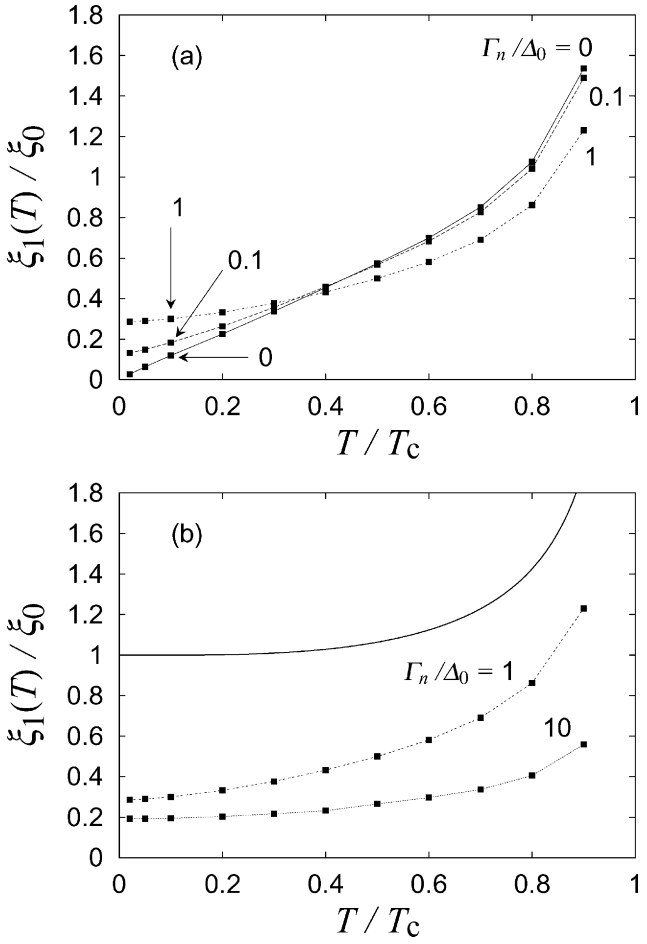

Fig. 1. The vortex core radius $\xi_1(T)$ (points) in the case of the s-wave vortex (20) as a function of the temperature T for several values of the impurity scattering rate $\Gamma_{\rm n}$. Lines are guides for the eye, except for the solid line in (b). In the plots, ξ_1 and T are normalized by ξ_0 and $T_{\rm c}$, respectively. Here, $T_{\rm c}$ is the superconducting critical temperature, ξ_0 is defined as $\xi_0 = v_{\rm F}/\Delta_0$, and Δ_0 is the BCS gap amplitude at zero temperature in the absence of impurities. (a) $\Gamma_{\rm n} = 0$, $0.1\Delta_0$, and Δ_0. (b) $\Gamma_{\rm n} = \Delta_0$ and $10\Delta_0$. The solid line in (b) is a plot of the function, $1/\tanh(1.74\sqrt{(T_{\rm c}/T)-1}) \approx \Delta_0/\Delta_{\rm BCS}(T) = v_{\rm F}/\Delta_{\rm BCS}(T)\xi_0$, which reproduces approximately the temperature dependence of the clean-limit BCS coherence length.

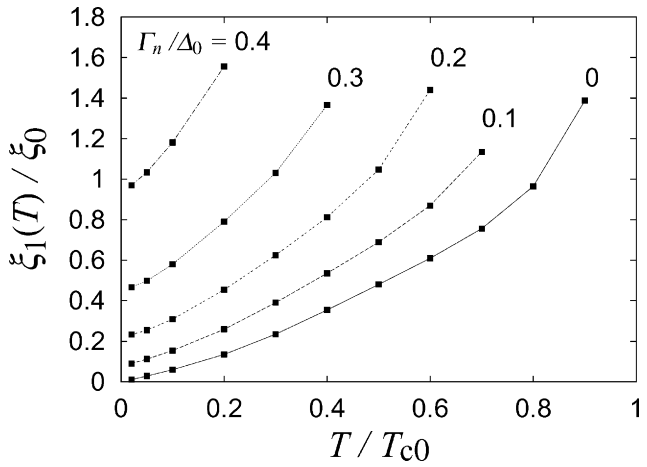

Fig. 2. The vortex core radius $\xi_1(T)$ (points) in the case of the chiral *positive* p-wave vortex (23) as a function of the temperature T for several values of the impurity scattering rate Γ_n. Lines are guides for the eye. In the plot, ξ_1 and T are normalized by ξ_0 and T_{c0}, respectively. Here, T_{c0} is the superconducting critical temperature in the absence of impurities, ξ_0 is defined as $\xi_0 = v_F/\Delta_0$, and Δ_0 is the BCS gap amplitude at zero temperature in the absence of impurities.

with a dirty limit result reported by Volodin *et al.*[19] Note that the overall temperature dependence of ξ_1 in the dirty case is quantitatively different from that of Ref. 19 ($\xi_{\rm eff}$), which is probably caused by the difference of the definitions of the vortex core radius. As displayed in Fig. 1(a) for the moderately clean case ($\Gamma_n = 0.1\Delta_0$, i.e., $l = 5\xi_0$) and even in the relatively dirty case ($\Gamma_n = \Delta_0$, i.e., $l = 0.5\xi_0$), the vortex core radius $\xi_1(T)$ shrinks approximately linearly in T with moderate curvature below $T \sim 0.6T_c$ and saturates towards a finite value in zero-temperature limit. This gradual saturation due to impurities is in contrast to a sudden truncation of the KP effect which happens below a certain temperature related to the discrete energy levels of the low-lying vortex bound states.[20,21]

4.2. Chiral P-Wave Vortices

In the chiral p-wave superconductors and generally in unconventional superconductors, the superconducting critical temperature decreases in the

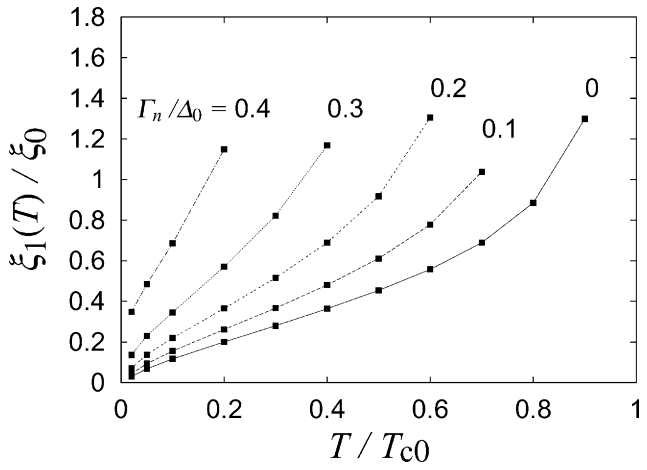

Fig. 3. The vortex core radius $\xi_1(T)$ (points) in the case of the chiral *negative* p-wave vortex (22) as a function of the temperature T for several values of the impurity scattering rate $\Gamma_{\rm n}$. Lines are guides for the eye. In the plot, ξ_1 and T are normalized by ξ_0 and $T_{\rm c0}$, respectively. Here, $T_{\rm c0}$ is the superconducting critical temperature in the absence of impurities, ξ_0 is defined as $\xi_0 = v_{\rm F}/\Delta_0$, and Δ_0 is the BCS gap amplitude at zero temperature in the absence of impurities.

presence of impurities. The units of the temperature T in Figs. 2 and 3 is $T_{\rm c0}$ (the superconducting critical temperature in the absence of impurities). We obtain ξ_1 from the dominant components $\Delta_+^{(\rm n,p)}(r)$ in Eqs. (22) and (23).

We show in Fig. 2 the vortex core radius $\xi_1(T)$ in the case of the positive vortex $\Delta^{(\rm p)}$ [Eq. (23)]. At low temperatures, $\xi_1(T)$ shrinks approximately linearly in T with moderate curvature and saturates towards a finite value in zero-temperature limit, as in the case of the s-wave vortex. The vortex core radius ξ_1 expands with the increase of $\Gamma_{\rm n}$, owing to the increase of the coherence length ξ with the suppression of the pair potential far away from the vortex core.

Figure 3 displays $\xi_1(T)$ for the negative vortex $\Delta^{(\rm n)}$ [Eq. (22)]. In contrast to the cases of the s-wave vortex and the positive vortex, the vortex core radius $\xi_1(T)$ strongly decreases even in the presence of impurities, and shrinks toward almost zero for the moderately clean cases below $\Gamma_{\rm n} \sim 0.2\Delta_0$.

We can understand, in the following way, the reason why the vortex core shrinkage is robust against impurities. In the Eilenberger equations (3)

and (8), the term which includes the impurity self energy is written as

$$[\hat{\sigma}, \hat{g}] = [\hat{\Sigma}, \hat{g}] = \frac{n_{\rm i} N_0 v^2}{D} [\langle \hat{g} \rangle, \hat{g}], \tag{44}$$

where we referred to Eqs. (7) and (12). Therefore, if the Fermi-surface-averaged Green function $\langle \hat{g} \rangle$ is equivalent to the original Green function $\hat{g}$ (namely, if $\langle \hat{g} \rangle = \hat{g}$), the above term (44) becomes zero and the impurity does not play a role in the Eilenberger equation. Such a special situation occurs in the negative vortex (22) of the chiral p-wave phase, and not in the positive vortex (23) or other usual vortices.[47,48] It corresponds to a local restoration of the Anderson's theorem inside the vortex core.[44–50] This negative vortex (22) is more favorable energetically than the positive vortex (23) at least in the clean limit,[52] and therefore the negative vortex is likely to exist in the chiral p-wave superconductors.

5. SUMMARY

We investigated the temperature dependence of the vortex core radius $\xi_1(T)$ defined in Eq. (1), incorporating the effect of nonmagnetic impurities in the Born limit. The isolated single vortex in the isotropic two-dimensional system was considered for the s-wave pairing symmetry and the chiral p-wave pairing symmetry.

In the case of the s-wave vortex (20), as seen in Fig. 1, *at low temperatures* the vortex core radius ξ_1 *increases* with the increase of the impurity scattering rate $\Gamma_{\rm n}$ up to $\Gamma_{\rm n} \sim \Delta_0$ owing to the saturation of the KP effect due to impurities. In contrast to it, *at high temperatures* the vortex core radius ξ_1 *decreases* with the increase of $\Gamma_{\rm n}$ owing to the decrease of the coherence length ξ due to impurities. In the case of the s-wave vortex (20) of the moderately clean state ($\Gamma_{\rm n} = 0.1\Delta_0$, i.e., $l = 5\xi_0$) and of the relatively dirty state ($\Gamma_{\rm n} = \Delta_0$, i.e., $l = 0.5\xi_0$), as seen in Figs. 1(a), at low temperatures the vortex core radius $\xi_1(T)$ *shrinks approximately linearly in T with moderate curvature* and saturates towards a finite value in zero-temperature limit. This gradual saturation due to impurities is in contrast to a sudden truncation of the KP effect due to the discreteness in the energy spectrum of the low-lying vortex bound states.[20,21] In the case of the chiral p-wave pairing system, as seen in Fig. 2, for the positive vortex (23) the shrinkage of the vortex core radius $\xi_1(T)$ saturates towards a finite value in zero-temperature limit by impurity scattering, analogous to the s-wave vortex. For the negative vortex (22), however, the local restoration of the Anderson's theorem inside the vortex core[44–50] yields a KP effect little affected by impurity scat-

tering and, as seen in Fig. 3, the vortex core radius $\xi_1(T)$ *strongly shrinks linearly in* T *at low temperatures even in the presence of impurities.*

It would naturally be highly desirable to establish the KP effect experimentally beyond the present level. Our analysis shows that impurity scattering which is harmful for the KP effect in conventional superconductors, can under certain condition be harmless in a chiral p-wave superconductor, making this kind of system a good candidate for experimental tests. On the other hand, we expect that rather weak shrinkings of vortex core observed in $NbSe_2$ (Refs. 26,28–30) and $CeRu_2$ (Ref. 32) may be explained partly in terms of the impurity effect, i.e., the vortex core shrinkage approximately linear in T with moderate curvature and its saturation towards a finite value in zero-temperature limit (Fig. 1(a)). Rather large extrapolated values of the vortex core radius at zero temperature observed experimentally might be partly attributed to effects of multiple gaps. Finally, we mention a multi-gap effect on the KP effect. Our preliminary results for $r_0(T)$ in a two-gap model show that a contribution from the Fermi surface with a smaller gap to the total supercurrent density $j(r)$ around a vortex makes the position r_0, at which $|j(r)|$ has its maximum value, shift outward away from the vortex center $r = 0$, leading to a finite r_0 at zero temperature in spite of the clean limit.[41] Our detailed results for the KP effect in a two-gap superconductor will be reported elsewhere. Sr_2RuO_4 (Refs. 43,61,62) and $NbSe_2$ (Ref. 63) have multiple bands and may be effectively two-gap superconductors. MgB_2 is a typical two-gap superconductor.[64] Further investigations on the vortex core shrinkage in terms of the multi-gap effects are left for future experimental and theoretical studies.

ACKNOWLEDGMENTS

We would like to thank N. Schopohl, T. Dahm, and S. Graser for enlightening discussions. One of the authors (N.H.) is grateful for the support by 2003 JSPS Postdoctral Fellowships for Research Abroad. We acknowledge gratefully financial support from the Swiss Nationalfonds.

REFERENCES

1. E. H. Brandt, J. Vanacken, and V. V. Moshchalkov, *Physica C* **369**, 1 (2002); G. E. Volovik, *J. Low Temp. Phys.* **121**, 357 (2000).
2. M. M. Salomaa and G. E. Volovik, *Rev. Mod. Phys.* **59**, 533 (1987).
3. G. Blatter, M. V. Feigel'man, V. B. Geshkenbein, A. I. Larkin, and V. M. Vinokur, *Rev. Mod. Phys.* **66**, 1125 (1994).

4. E. H. Brandt, *Rep. Prog. Phys.* **58**, 1465 (1995).
5. L. Kramer and W. Pesch, *Z. Phys.* **269**, 59 (1974).
6. S. G. Doettinger, R. P. Huebener, and S. Kittelberger, *Phys. Rev. B* **55**, 6044 (1997).
7. C. Caroli, P. G. de Gennes, and J. Matricon, *Phys. Lett.* **9**, 307 (1964).
8. H. F. Hess *et al.*, *Phys. Rev. Lett.* **62**, 214 (1989); *Phys. Rev. Lett.* **64**, 2711 (1990); Ch. Renner *et al.*, *Phys. Rev. Lett.* **67**, 1650 (1991).
9. F. Gygi and M. Schlüter, *Phys. Rev. B* **43**, 7609 (1991).
10. N. Schopohl and K. Maki, *Phys. Rev. B* **52**, 490 (1995).
11. D. Rainer, J. A. Sauls, and D. Waxman, *Phys. Rev. B* **54**, 10094 (1996).
12. N. Hayashi, M. Ichioka, and K. Machida, *Phys. Rev. Lett.* **77**, 4074 (1996); *Phys. Rev. B* **56**, 9052 (1997); *J. Phys. Soc. Jpn.* **67**, 3368 (1998), eprint cond-mat/9807253.
13. Y. Tanaka, A. Hasegawa, and H. Takayanagi, *Solid State Commun.* **85**, 321 (1993); S. M. M. Virtanen and M. M. Salomaa, *Phys. Rev. B* **60**, 14581 (1999); *Physica B* **284-288**, 741 (2000).
14. G. E. Volovik, *JETP Lett.* **58**, 455 (1993).
15. W. Pesch and L. Kramer, *J. Low Temp. Phys.* **15**, 367 (1974); L. Kramer, W. Pesch, and R. J. Watts-Tobin, *J. Low Temp. Phys.* **14**, 29 (1974).
16. E. H. Brandt, *Phys. Status Solidi B* **77**, 105 (1976); see also Sec. 1.4 of Ref. 4.
17. J. Rammer, W. Pesch, and L. Kramer, *Z. Phys. B: Condens. Matter* **68**, 49 (1987).
18. M. Ichioka, N. Hayashi, N. Enomoto, and K. Machida, *Phys. Rev. B* **53**, 15316 (1996).
19. A. P. Volodin, A. A. Golubov, and J. Aarts, *Z. Phys. B* **102**, 317 (1997); an experimental result by STM is also given therein.
20. N. Hayashi, T. Isoshima, M. Ichioka, and K. Machida, *Phys. Rev. Lett.* **80**, 2921 (1998).
21. M. Kato and K. Maki, *Prog. Theor. Phys.* **103**, 867 (2000), eprint cond-mat/0004370.
22. M. Kato and K. Maki, *Europhys. Lett.* **54**, 800 (2001); *Prog. Theor. Phys.* **107**, 941 (2002); *Physica B* **312-313**, 47 (2002); eprint cond-mat/0011173; the temperature dependence of the vortex core radius is investigated therein for the d-wave superconductors in the quantum limit.
23. Y. Kato and N. Hayashi, *J. Phys. Soc. Jpn.* **70**, 3368 (2001), eprint cond-mat/0107517.
24. Ø. Elgarøy, eprint cond-mat/0111440; N. Nygaard, G. M. Bruun, C. W. Clark, and D. L. Feder, *Phys. Rev. Lett.* **90**, 210402 (2003).
25. F. V. de Blasio and Ø. Elgarøy, *Phys. Rev. Lett.* **82**, 1815 (1999); Ø. Elgarøy and F. V. de Blasio, *Astron. Astrophys.* **370**, 939 (2001), eprint astro-ph/0102343.
26. For a latest review, J. E. Sonier, *J. Phys.: Condens. Matter* **16**, S4499 (2004), eprint cond-mat/0404115.
27. Yu. N. Ovchinnikov, *Z. Phys. B* **27**, 239 (1977).
28. J. E. Sonier, J. H. Brewer, and R. F. Kiefl, *Rev. Mod. Phys.* **72**, 769 (2000).
29. J. E. Sonier *et al.*, *Phys. Rev. Lett.* **79**, 2875 (1997).
30. R. I. Miller *et al.*, *Phys. Rev. Lett.* **85**, 1540 (2000).
31. A. Yaouanc, P. Dalmas de Réotier, and E. H. Brandt, *Phys. Rev. B* **55**, 11107

(1997).
32. R. Kadono *et al.*, *Phys. Rev. B* **63**, 224520 (2001).
33. A. A. Golubov and U. Hartmann, *Phys. Rev. Lett.* **72**, 3602 (1994).
34. M. Ichioka, A. Hasegawa, and K. Machida, *Phys. Rev. B* **59**, 184 (1999); *Phys. Rev. B* **59**, 8902 (1999).
35. P. Miranović, M. Ichioka, and K. Machida, *Phys. Rev. B* **70**, 104510 (2004).
36. V. G. Kogan and N. V. Zhelezina, eprint cond-mat/0407673.
37. J. E. Sonier *et al.*, *Phys. Rev. Lett.* **79**, 1742 (1997); *Phys. Rev. Lett.* **93**, 017002 (2004).
38. M. Fogelström and J. Kurkijärvi, *J. Low Temp. Phys.* **98**, 195 (1995).
39. R. Kadono *et al.*, *Phys. Rev. B* **69**, 104523 (2004); M. Takigawa, M. Ichioka, and K. Machida, *J. Phys. Soc. Jpn.* **73**, 450 (2004), eprint cond-mat/0303541.
40. A. E. Koshelev and A. A. Golubov, *Phys. Rev. Lett.* **90**, 177002 (2003).
41. N. Hayashi, Y. Kato, and M. Sigrist, in preparation.
42. T. M. Rice and M. Sigrist, *J. Phys.: Condens. Matter* **7**, L643 (1995); M. Sigrist *et al.*, *Physica C* **317-318**, 134 (1999).
43. A. P. Mackenzie and Y. Maeno, *Rev. Mod. Phys.* **75**, 657 (2003).
44. G. E. Volovik, *JETP Lett.* **70**, 609 (1999); eprint cond-mat/9709159.
45. Y. Kato, *J. Phys. Soc. Jpn.* **69**, 3378 (2000), eprint cond-mat/0009296.
46. Y. Kato and N. Hayashi, *J. Phys. Soc. Jpn.* **71**, 1721 (2002), eprint cond-mat/0203271.
47. N. Hayashi and Y. Kato, *Physica C* **367**, 41 (2002); *Phys. Rev. B* **66**, 132511 (2002).
48. N. Hayashi and Y. Kato, *J. Low Temp. Phys.* **130**, 193 (2003), eprint cond-mat/0210642.
49. Y. Kato and N. Hayashi, *Physica C* **388-389**, 519 (2003).
50. M. Matsumoto and M. Sigrist, *Physica B* **281-282**, 973 (2000).
51. M. Matsumoto and R. Heeb, *Phys. Rev. B* **65**, 014504 (2002).
52. R. Heeb and D. F. Agterberg, *Phys. Rev. B* **59**, 7076 (1999).
53. A. Tanaka and X. Hu, *Phys. Rev. Lett.* **91**, 257006 (2003).
54. Q. Han, Z. D. Wang, Q.-H. Wang, and T. Xia, *Phys. Rev. Lett.* **92**, 027004 (2004).
55. G. Eilenberger, *Z. Phys.* **214**, 195 (1968); A. I. Larkin and Yu. N. Ovchinnikov, *Zh. Éksp. Teor. Fiz.* **55**, 2262 (1968), [*Sov. Phys. JETP* **28**, 1200 (1969)]; J. W. Serene and D. Rainer, *Phys. Rep.* **101**, 221 (1983).
56. H. Kusunose, *Phys. Rev. B* **70**, 054509 (2004); the derivation of the quasiclassical equations is concisely summarised therein.
57. E. V. Thuneberg, J. Kurkijärvi, and D. Rainer, *Phys. Rev. B* **29**, 3913 (1984); *J. Phys. C: Solid State Phys.* **14**, 5615 (1981).
58. N. Schopohl, eprint cond-mat/9804064.
59. M. Eschrig, Ph.D. Thesis, University of Bayreuth, 1997; H. Eschrig, *Optimized LCAO Method and the Electronic Structure of Extended Systems* (Springer-Verlag, Berlin, 1989), Sec. 7.4.
60. M. Tinkham, *Introduction to Superconductivity, 2nd Ed.* (McGraw-Hill, New York, 1996).
61. D. F. Agterberg, T. M. Rice, and M. Sigrist, *Phys. Rev. Lett.* **78**, 3374 (1997).
62. H. Kusunose, *J. Phys. Soc. Jpn.* **73**, 2512 (2004), eprint cond-mat/0405631.

63. E. Boaknin *et al.*, *Phys. Rev. Lett.* **90**, 117003 (2003).
64. H. J. Choi *et al.*, *Nature* **418**, 758 (2002); N. Nakai *et al.*, *J. Phys. Soc. Jpn.* **71**, 23 (2002), eprint cond-mat/0111088; S. Tsuda *et al.*, *Phys. Rev. Lett.* **91**, 127001 (2003); T. Dahm and N. Schopohl, *Phys. Rev. Lett.* **91**, 017001 (2003); A. Shibata *et al.*, *Phys. Rev. B* **68**, 060501 (2003); T. Dahm, eprint cond-mat/0410158.